VERIFICATION OF AN EMPIRICAL DAMAGE TOLERANCE METHOD

David O. Adams, Douglas E. Tritsch, and Rolf R. Paulson

Sikorsky Aircraft Corporation
6900 N. Main Street, Stratford, Connecticut 06615-9129 USA
doadams@sikorsky.com, dtritsch@sikorsky.com, rpaulson@sikorsky.com

Key words: ERF32, rotorcraft, CH-53K, damage tolerance

Abstract: The use of damage tolerance methodology to manage flight-critical helicopter dynamic components by periodic inspections for propagating cracks is increasing, and certifying agencies are asking for more attention to this methodology. One example of this is the U.S. Marine Corps CH-53K Heavy Lift helicopter program, where consideration of Damage Tolerance is required in the design and fatigue testing of dynamic components. However, previous crack propagation test programs required an effort based on analysis to account for different load spectrums. An independent test-based method for crack propagation substantiations, based on the "Paris Law" in fracture mechanics, has been previously proposed by the authors. The method appeared workable; however, a full-scale calibration, or verification, was needed to show that in fact a test result at one load spectrum could be used to predict the results for another load spectrum. Consequently, a series of tests were conducted as part of the Risk Reduction phase of the CH-53K program. Aluminum and titanium test specimens were designed to represented rotor-type components and were subjected to crack propagation testing at various load levels. The results showed that the empirical damage tolerance method was valid. However, scatter in the results was observed, which are attributed to variations in material da/dN characteristics. A comparison to a pure analytical approach for these same specimens was conducted. Finally the program also provided valuable experience with the problems and difficulties in obtaining good crack propagation test data on full-scale helicopter components.

Figure 1: U.S. Marine Corps CH-53K Helicopter

Presented at the 32nd European Rotorcraft Forum, Maastricht, Netherlands, September 2006

1 INTRODUCTION

1.1 The need for an Empirical Damage Tolerance method

Damage Tolerance methodology producing inspection intervals based on crack growth characteristics has been in use on flight critical helicopter dynamic components since about 1960, but only in a limited number of applications. It was called "fail-safe" methodology in those days. At Sikorsky the substantiation of such a component consists of a full-scale crack propagation spectrum test program that results in the determination of safe inspection intervals. The applications have been previously limited in number because helicopter high cycle rates and the need for difficult inspections frequently requiring disassembly usually resulted in impractical and unworkable maintenance requirements. However, it is inevitable that the difficulties currently inhibiting the widespread use of Damage Tolerance will be overcome. Advances such as indirect inspection methods, global inspections methods, built-in damage detection devices, usage monitoring, improved analysis tools, and better materials will all contribute to the future success of this methodology.

Along those lines, requirements for the U.S. Marine Corps CH-53K Heavy Lift helicopter, Figure 1, include damage tolerance evaluations for all critical modes on all dynamic components. This evaluation will be primarily analytical, but full-scale crack propagation test data for analytical correlation will also be obtained on many of these components in conjunction with the planned Flaw Tolerant Safe-Life fatigue test program. Damage Tolerance is also available as an alternate management method for CH-53K dynamic components when needed.

Use of analysis alone for the substantiation of a crack growth and inspection approach for helicopter dynamic components is not considered to provide reliable and consistent results with known conservative margins in every case. This difficulty is illustrated in Reference 1. The importance of good analysis tools and methods in providing an initial component design and configuration with a high probability of success is not minimized; however, the analysis is not ready to stand on its own for routine substantiations for general service use.

A substantiation method based solely on full-scale fatigue test results and providing high-confidence high-reliability inspection intervals is needed if damage tolerance is to be used to manage flight-critical fatigue loaded components in service. In addition, the method must employ a systematic approach producing a unique result, and be straightforward to implement in the test lab, in flight test, and in the damage calculation. The attributes needed are present in our familiar safe-life fatigue test substantiations, namely: completely independent of design analysis, use of an easily-measured Substantiating Parameter, multiple specimen full-scale fatigue testing, simple description of the component strength, easy incorporation of measured flight test loads and the customer's usage spectrum, and most importantly, no new testing required for loads and usage changes.

1.2 Proposed method

A method which meets the above requirements was formulated at Sikorsky and is described in Reference 2. This method employs curve fitting to the full-scale crack growth test data to derive factors for the following equation:

$$\frac{Da}{DN} = F\left(P_V \sqrt{a}\right)^{\phi} \qquad (1)$$

Where:

Da/DN is expressed with uppercase Ds to denote its experimental basis, and to not imply an understanding of infinitesimal crack growth.

a is the crack length and N is the number of cycles of applied load, expressed in millions.

F is a constant derived from curve fitting full-scale test data.

P_V is the vibratory Substantiating Parameter, half of the peak-to-peak variation in the applied flight test or bench test substantiating load. $P_V = 1.0$ is set at some reference value of the applied load.

ϕ is a constant derived from curve fitting full-scale test data.

This relationship is a modification of the Paris Law in fracture mechanics, Reference 3. The modification replaces the stress range parameter with a normalized Substantiating Parameter, P_V, which is easily and reliably measured in ground test and flight test and is shown to be proportional to the stress in the field near the propagating crack. The Paris Law geometry factor variation is assumed to be contained in the shape of the test propagation curve, divided into segments if needed. The factor F contains all of the proportionality factors and constants, and the factor ϕ replaces the Paris exponent.

Curve fitting consists of finding an exponent that matches the curvature, and then moving the fitted line with different F (life) factors to match the test data. The curve fit line is produced by a numerical integration of the EDT equation with each set of trial factors. When multiple loads are included, as with a spectrum test or when calculating for a service spectrum, the integration uses each load condition weighted by its loading frequency.

Applications of the curve fitting idea were tried with good results for several full-scale crack propagation data sets as reported in Reference 2.

1.3 The need for a "calibration" of the method

None of the full-scale data available for the Reference 2 work contained multiple specimen testing conducted at different load spectrums. Coupon work was not considered appropriate for this because of the importance of full-scale geometry in the determination of crack growth characteristics. So the ability of the EDT method to successfully predict the results for a given set of loads based on the tests conducted at a different set of loads was not demonstrated.

Because of the potential significant contribution of the EDT method to the CH-53K, Naval Air Systems Command included a crack propagation analysis and test program in the Risk Reduction phase of that program. The intent of the program was to verify the ability of the EDT method to establish an inspection program for service use based on a limited fatigue test data base. This paper shows the results of that program.

2. DESIGN AND ANALYSIS OF TEST SPECIMENS

2.1 Test specimen configuration

The specimen design was intended to simulate a "rotor" type component as opposed to an "airframe" type component. It reacts a significant axial load and creates a bending stress by an offset of the axial load and an asymmetrical cross-section as shown in Figure 2 below. This dual loading approach is somewhat different than standard material testing.

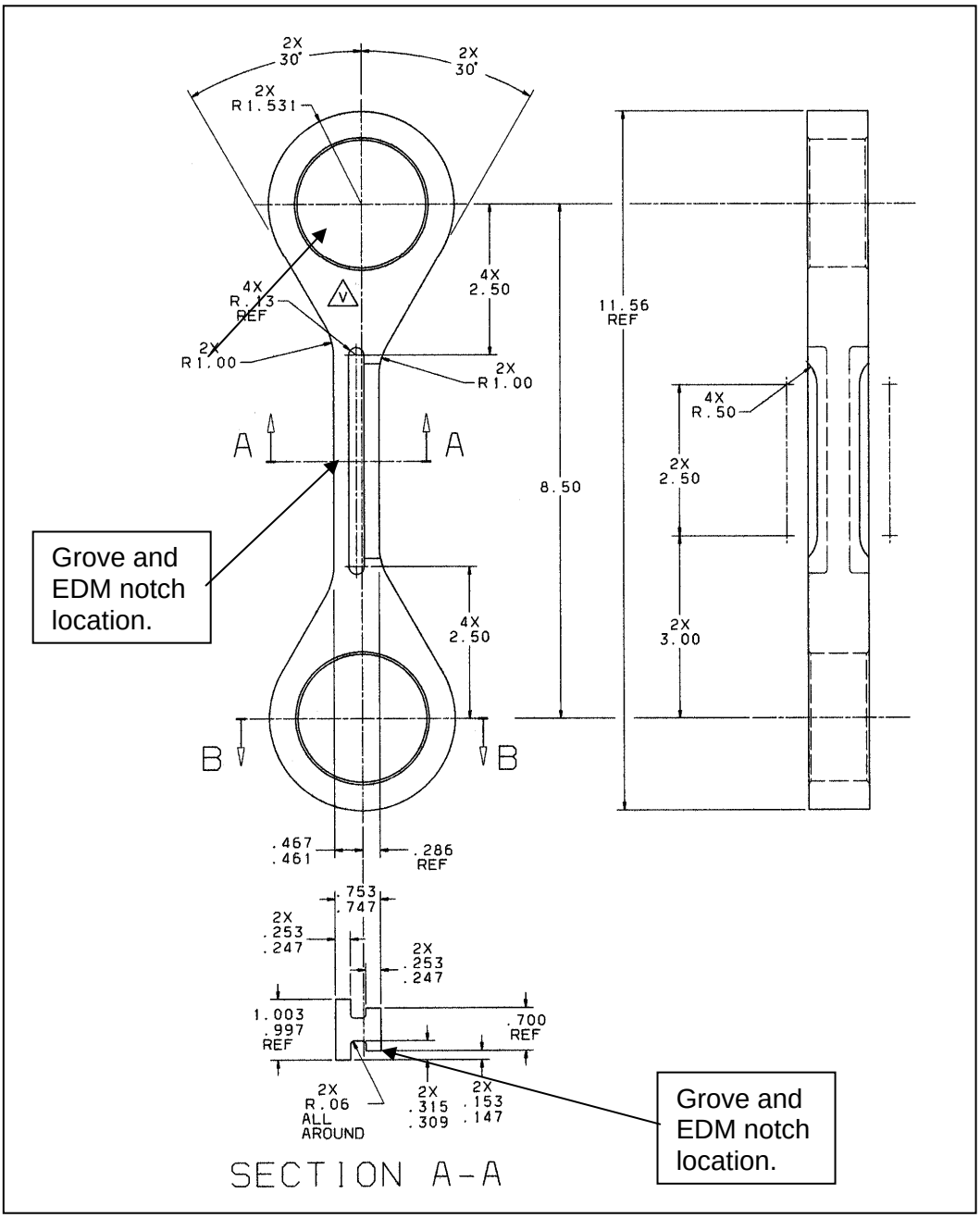

Figure 2: Test Specimen Details, Dimensions in Inches.

A single axial load was applied through spherical bearings installed in the specimen loops, not shown in the figure. An EDM notch was imposed at the desired initial crack location at a front corner at midspan. However, Specimen 1 failed in chafing at the bearing bore. All subsequent specimens incorporated a machined groove with a radius of .035 inches on the

side of the specimen's front section. This groove created a stress concentration of ~2.7. The EDM notch was applied at the front corner of this groove.

The materials chosen for this evaluation are 7075-T7351 aluminum and 6AL-4V STOA Titanium, which are representative of materials which will be used in CH-53K rotor components. The specimen cross-section was chosen because it is not simple to analyze when combined with the combined bending and axial load distribution. Loads were chosen to provide stress levels representative of CH-53K rotor components.

3. CRACK PROPAGATION TEST PROGRAM

3.1 EDM notching

An EDM (Electrical Discharge Machining) notch was placed on each specimen at the location shown in Figure 2. The set-up for the EDM cut is shown in Figure 3. A boroscope with a video camera was used to assure positioning of the EDM cut at the 9 o'clock position. The EDM electrode was a copper-tungsten foil 0.003 inch thick. Only the very center of the electrode discharges on the corner of the test specimen. The foil was sharpened to a knife edge using 400 grit sandpaper. On the aluminum specimens very little of the electrode was consumed during the EDM process, allowing the notch to be very sharp. When cutting the titanium specimens, the EDM electrode was consumed ~0.0015" for a 0.005" deep cut. This required the foil to be re-sharpened after each specimen was cut. Figure 4 shows a close-up view of an EDM cut. The cut is located on the corner of the machined notch and is.0065" long on the front of the specimen.

Figure 3: EDM Notching Set-up

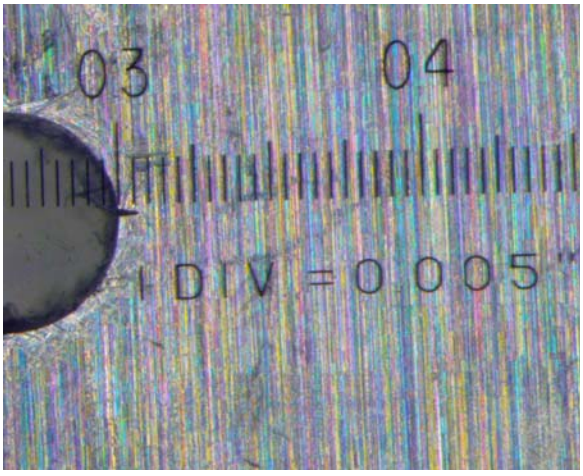

Figure 4: Typical EDM Notch

3.2 Specimen instrumentation

Eleven strain gages were placed on the front and back of the specimen's central section for correlation and surveys as shown in Figure 5.

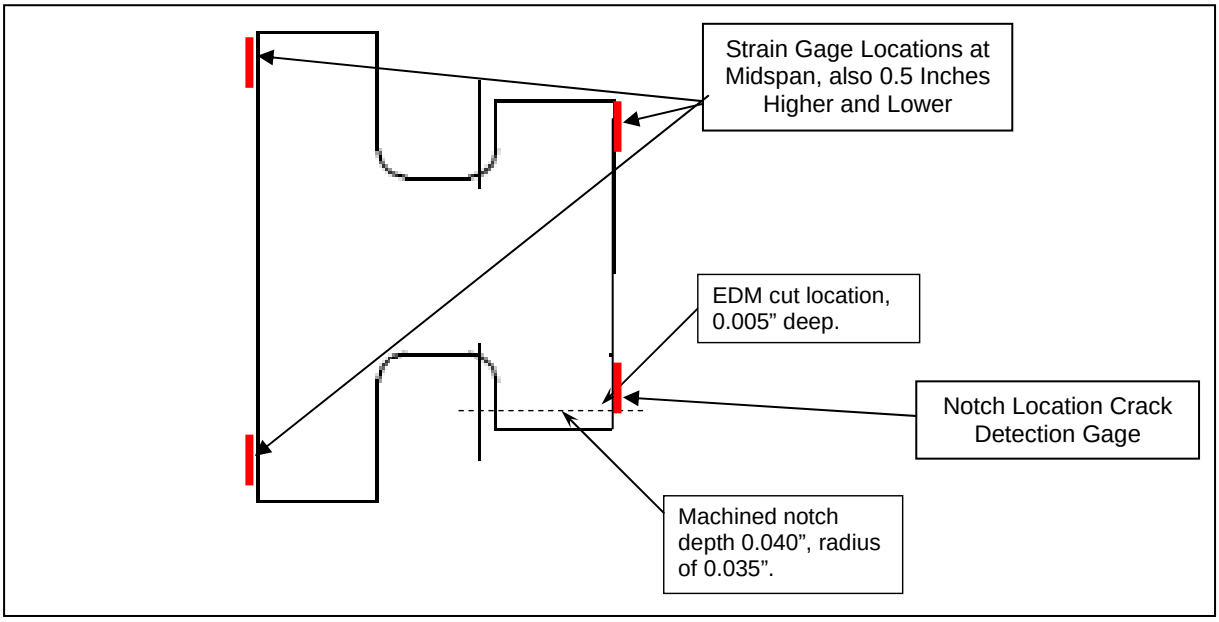

Figure 5: Cross-Section Strain Gage and Crack Detection Gage Locations

A crack detection gage was positioned at the tip of the EDM notch on each specimen as shown in Figure 5. When a crack initiates, the foil filament is broken causing an open circuit and triggering a test shutdown. A soluble glue, Loctite 404, was used to attach the crack detection gage. The soluble glue was used since it was desired to be able to clean and polish the face after crack initiation for better observation of the crack tip and crack length measurement under a microscope. After initiation, the gage was removed and the glue was removed using Loctite X-NMS cleanup solvent. The faces of the specimens were polished to a glossy finish using 1 micron diamond paste after crack initiation.

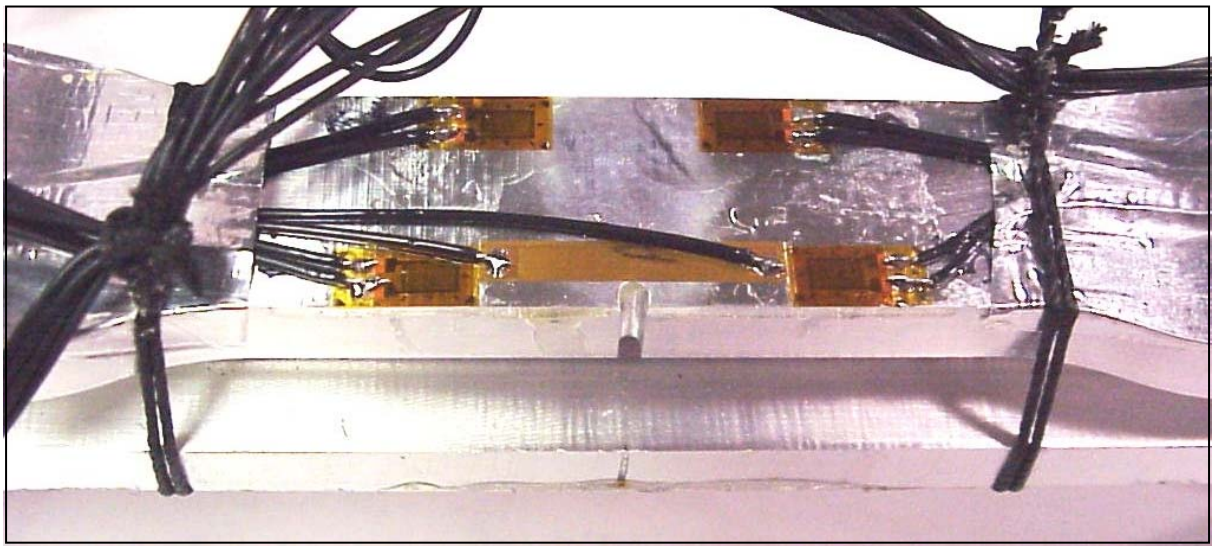

Figure 6: Crack Detection Gage Installation

This approach, however, did not produce an adequate bond for the crack detection gage on the aluminum specimens, and early detection of the crack initiation was not achieved. Good results were obtained on the titanium specimens. This is attributed to the ability to etch the surface of the titanium adequately with Kroll's Etch. This was not achievable on the aluminum.

For testing of full-scale helicopter components, the ability to very accurately measure the crack length by microscope is not necessarily required, and so the detailed cleaning and polishing is not required. In that case, an epoxy adhesive such as is used for installation of strain gages will provide a good bond and early crack detection. Subsequent measuring of propagating crack length can be accomplished by appropriate NDI procedures such as aided visual, dye penetrant or eddy-current inspections.

3.3 Test conduct

Testing was conducted on a servo-hydraulic MTS fatigue machine with a capacity of 20,000 lbs. The specimen ends were held in a clevis with a one inch diameter pin through the spherical bearing. There was a small amount of pivoting about the lubricated pin due to the off-axis loading. There was no observed motion in the spherical bearing until the crack became quite long and significant bending deflection occurred. All testing was conducted at a frequency of 15 Hz.

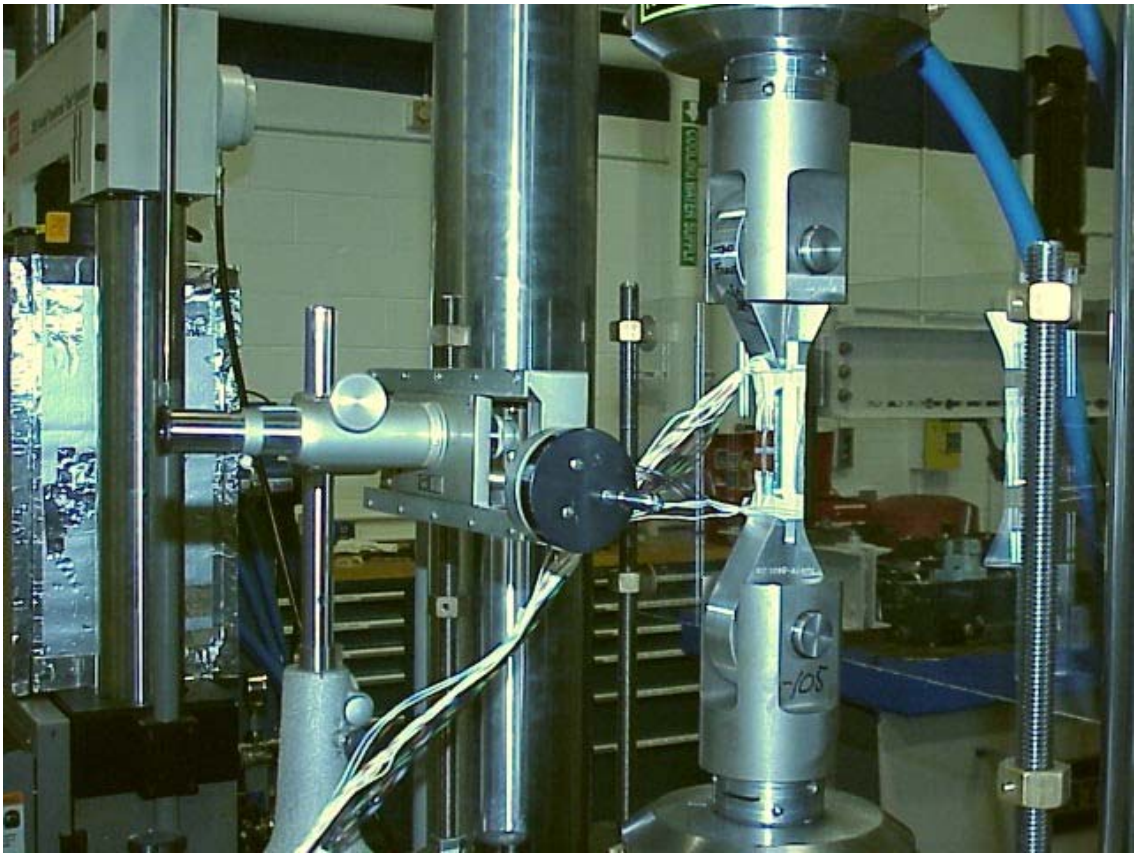

Figure 6: Crack Propagation Test Set-up

Some difficulty was encountered in obtaining the desired loading on the crack face, especially with the titanium specimens. The pivot bearing arrangement used here offers simplicity, but rotation of the pin and bearing may have been restricted, especially at small crack lengths, changing the load distribution. Independent control over the bending and axial loads is seen

to be a much better approach, and is more typical of the test set-up for a full-scale helicopter component.

The crack detection gage was used to stop the test as soon as initiation had occurred. There were inconsistent results in catching the crack short for the aluminum specimens due to the poor bond of the detection gage to the specimen face. The titanium results were much better.

The loads required to initiate the crack were generally higher than the loads eventually used to propagate the crack. Table 1 summarizes the crack initiation and crack propagation test loading, and the initial crack sizes for each specimen.

Table 1: Specimen Loading Conditions

Specimen S/N	Max Initiation Load (lb)	Crack Propagation Loads (lb)			Initiation Cycles (10^6)	Initial Crack Length (inch)*
		Max	Min	P_V		
Al-2	2500	2500	250	1.0	1.195	0.071
Al-3	3500	3000	300	1.2	2.00	0.059
Al-4	3500	1500	150	0.60	0.748	0.291
Al-5	3500	2500	250	1.0	0.858	0.252
Al-6	5,000	Spectrum Test**			0.393	0.196
Ti-1	18,000	11290	1129	1.129	0.043	0.020
Ti-2	15,000	10000	1000	1.0	0.052	0.017
Ti-3	15,000	6690	669	0.669	0.044	0.026
Ti-4	15,000	10000	1000	1.0	0.064	0.015

*Crack length from end of EDM notch when first detected. Later corrected to edge distance.
**Spectrum Test Max Loads, all with R = .1, were 3000 lb for 5% time, 2500 for 20%, 2000 for 50%, and 1500 for 25%. Run in blocks of 5000 cycles.

After crack initiation, glue removal, and surface polishing, the crack was measured using a microscope with a travelling stage. The microscope provided 200X magnification to allow very accurate length measurements.

The crack initiation load was reduced to the planned propagation test load; however, the "counting" of propagation test cycles did not begin until some definite new growth of the crack occurred at the propagation test load. This was necessary to avoid unconservative dwell effects from the higher crack initiation load. Testing continued until specimen fracture under the propagation loading.

3.4 Crack Surface Evaluation

An evaluation of the crack surface features was conducted on one of the aluminum and one of the titanium specimens, shown below in Figures 7 and 8.

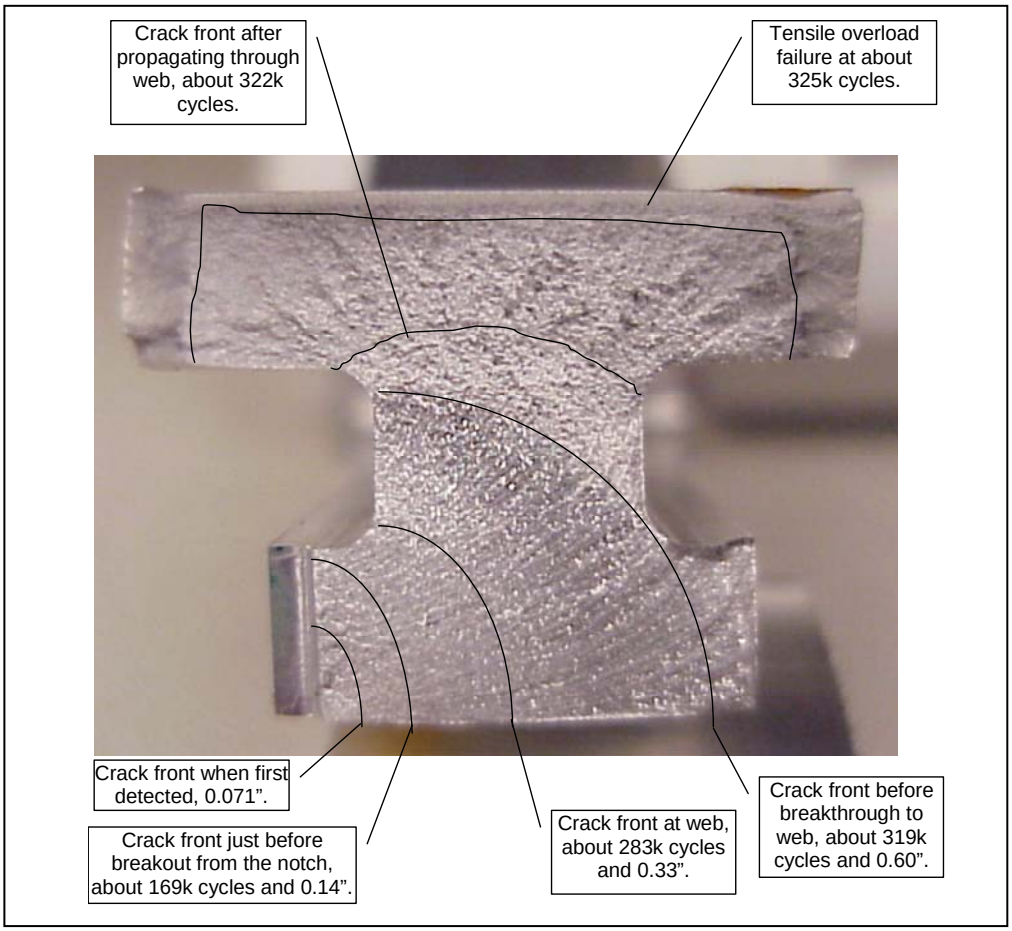

Figure 7: Aluminum Specimen Crackfront Evaluation

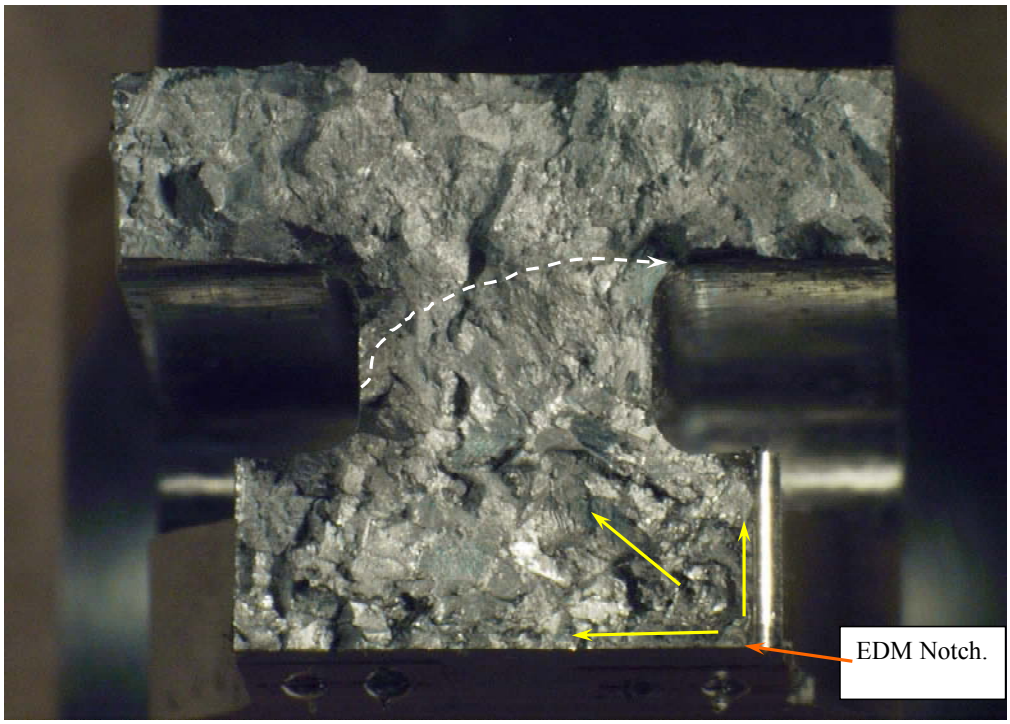

Figure 8: Titanium Specimen Crackfront Evaluation

Characteristically, the aluminum fracture surface is much easier to read than the titanium. Definite crackfront markings on the aluminum show how this simple cross section has at least 3 distinct zones of crack propagation, the last one being closest to the critical crack size. Only one distinct crackfront was found on the titanium specimen, as shown.

4. ANALYSIS OF TEST RESULTS

4.1 Strain surveys

The first step in understanding any fatigue test result is to check the validity of the selected substantiating parameter, in this case applied external load, which creates both an axial and bending stress field. The substantiating parameter must be linear with a local field stress in the area of the crack tip over the entire length of the crack. The proportionality factor can be different for each crack length, but still reasonably linear. This assures that the effect of different levels of the substantiating parameter, such as in a spectrum test or life calculation, have a proportional effect on the stress that drives the crack for all crack lengths.

Initial linearity was verified for both the aluminum and titanium specimens using applied load as the substantiating parameter and an average of 2 strain gages above and below the crack as the local field stress.

The proportionality question is addressed by examining the same average field stress as a function of crack length on specimens tested at different loads, as shown in Figure 9.

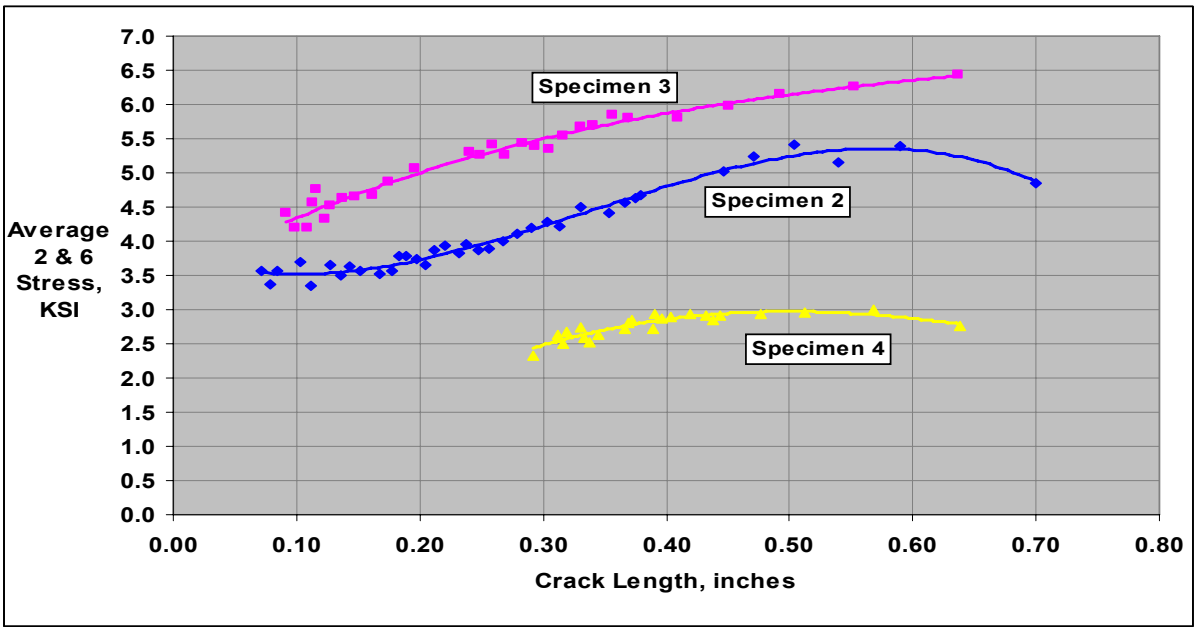

Figure 9: Aluminum Strain Variation with Crack Length and Load

For the aluminum specimens, the "baseline" load, Specimen 2, was 2500 lb peak (at R = .1 this is 1375 lb steady and 1125 lb vibratory). The substantiating parameter is normalized to this condition, i.e., $P_V = 1.0$. The "high" load condition selected for Specimen 3 was 3000 lb peak with R = .1, or $P_V = 1.20$, and the "low" load selected for Specimen 4 was 1500 lb peak with R = .1, or $P_V = .60$.

The strain variation shown above is somewhat complex, but can be normalized as a fraction of the Specimen 2 stress for each crack length, as shown below in Figure 10.

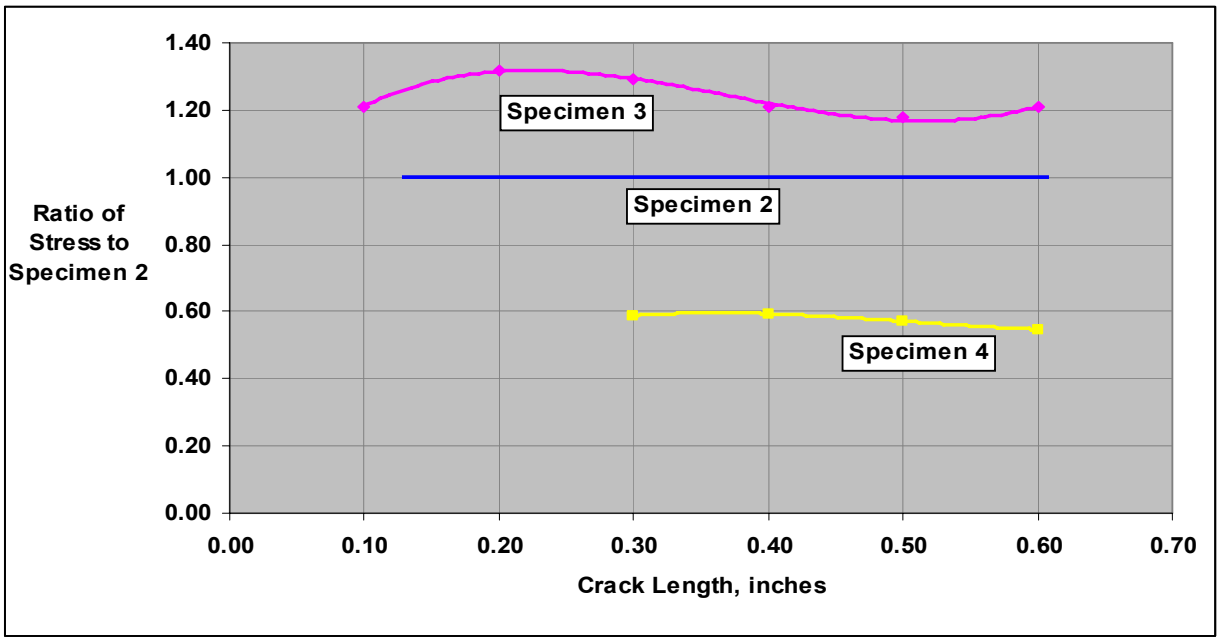

Figure 10: Normalized Aluminum Specimen Strain Variation

While this result is not as consistent as desired, and somewhat compromised by the large initial crack size on Specimen 4, the basic linearity premise is verified for the aluminum specimens. Specimen 3 operates at a 20% higher stress than the baseline Specimen 2 for most of its crack growth, and Specimen 4 operates at about 60% of the baseline stress, in proportion to the substantiating parameter.

The corresponding results for the Titanium specimens are shown below in Figures 11 and 12.

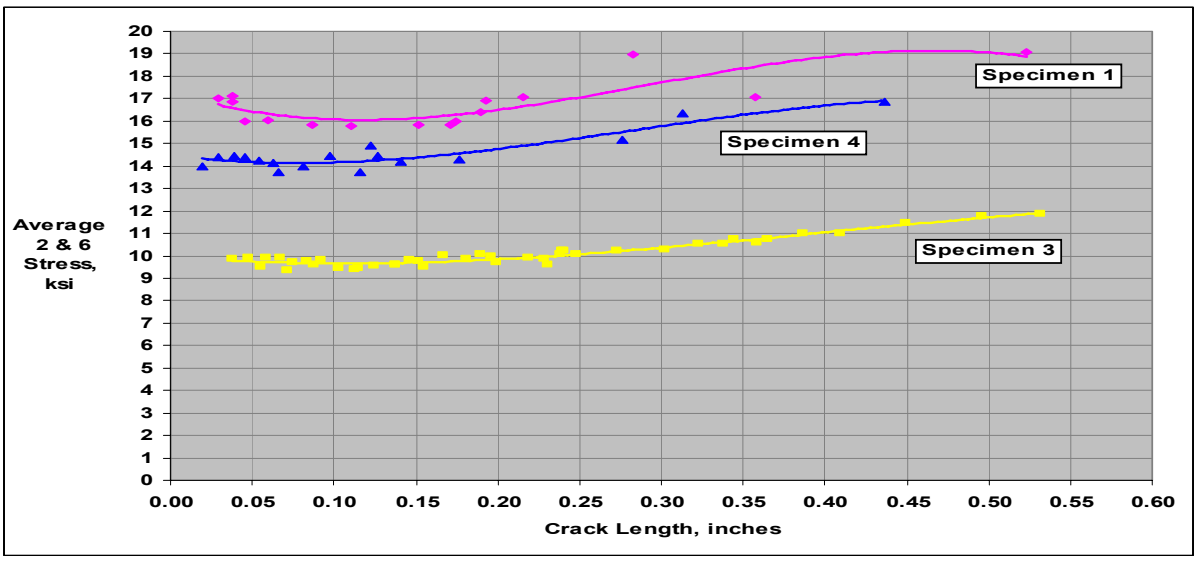

Figure 11: Titanium Strain Variation with Crack Length and Load

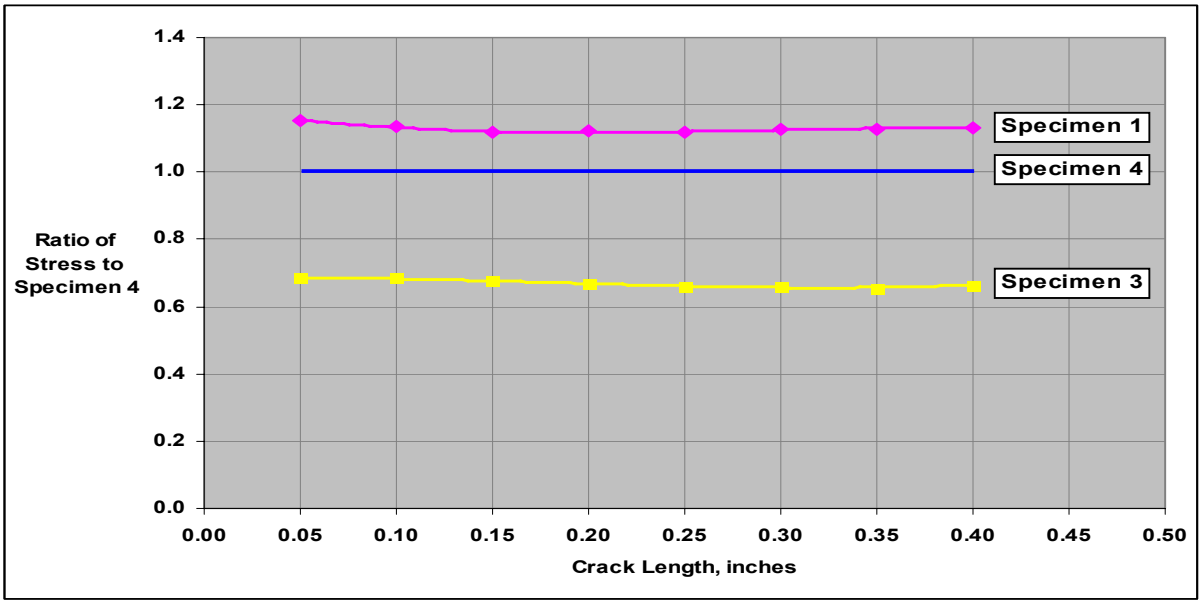

Figure 12: Normalized Titanium Specimen Strain Variation

In this case the local field stress is disproportionately low for both specimens over the crack length. While the applied load on Specimen 1 was 20% above the baseline, only 13% increase was seen in the local field stress near the crack. The applied load on Specimen 3 was 70% of the baseline, but 67% is seen in the field stress. Corrections are needed to provide an "equivalent" applied load that meets the proportionality requirement for a substantiating parameter. These corrections appear as the Crack Propagation loads for titanium in Table 1, and are used in the analysis that follows.

4.2 Aluminum crack propagation data

Crack length as a function of load cycles from crack detection was obtained from the aluminum specimens. However, crack length measurement from the root of the EDM notch resulted in some inconsistencies in the initial analysis of this data. Since the depth of the machined groove and the depth of the EDM notch were not precisely the same on each specimen, an alternate analysis was conducted with crack length based on the distance from the crack tip to the edge of the component. This approach provided more consistent results and is recommended as a standard practice. Figures 13-17 show the crack propagation data with the trial and error curve fit lines and corresponding EDT equation factors.

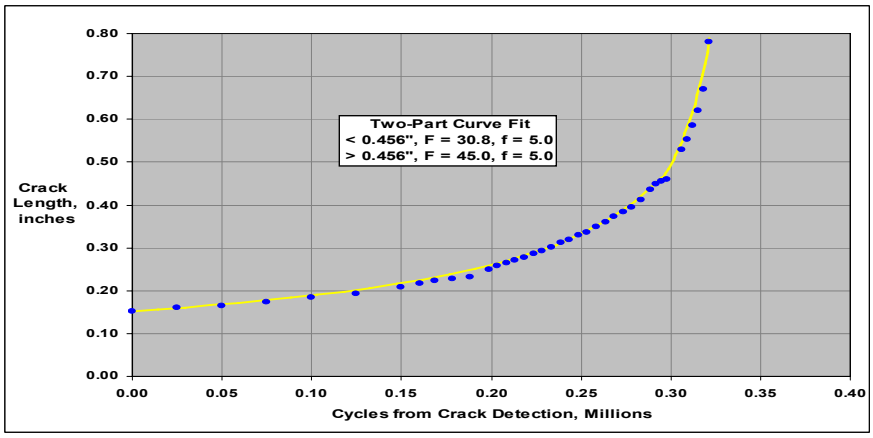

Figure 13: Aluminum Specimen 2 Crack Propagation Results

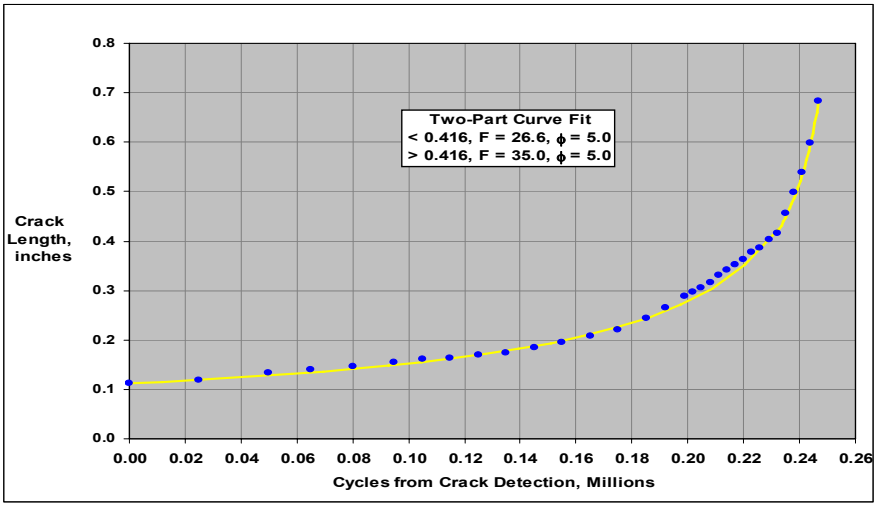

Figure 14: Aluminum Specimen 3 Crack Propagation Results

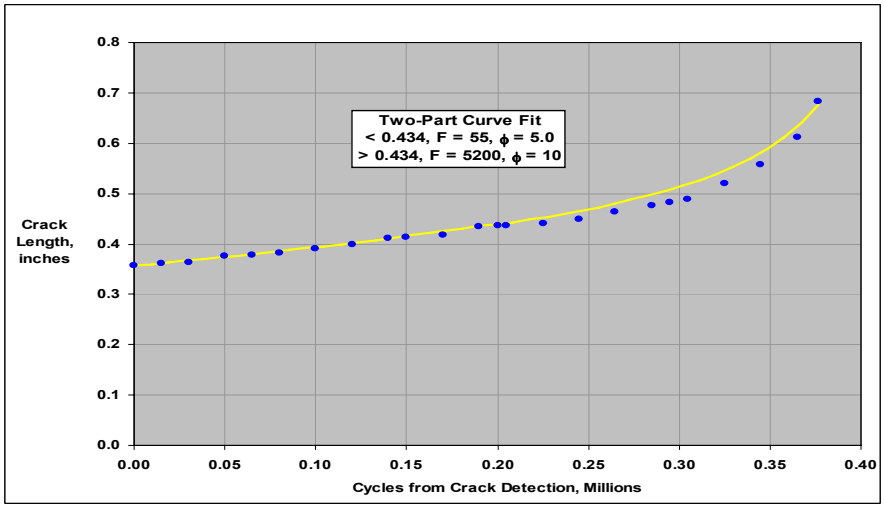

Figure 15: Aluminum Specimen 4 Crack Propagation Results

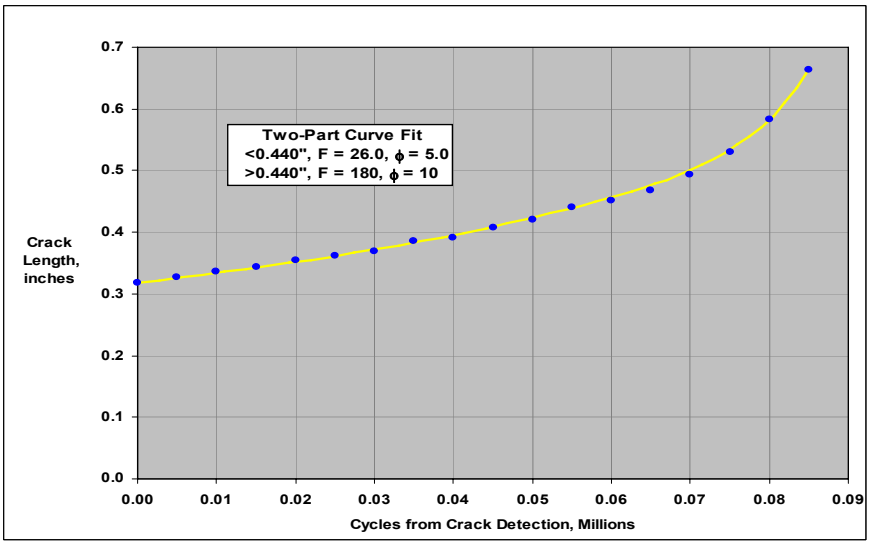

Figure 16: Aluminum Specimen 5 Crack propagation Results

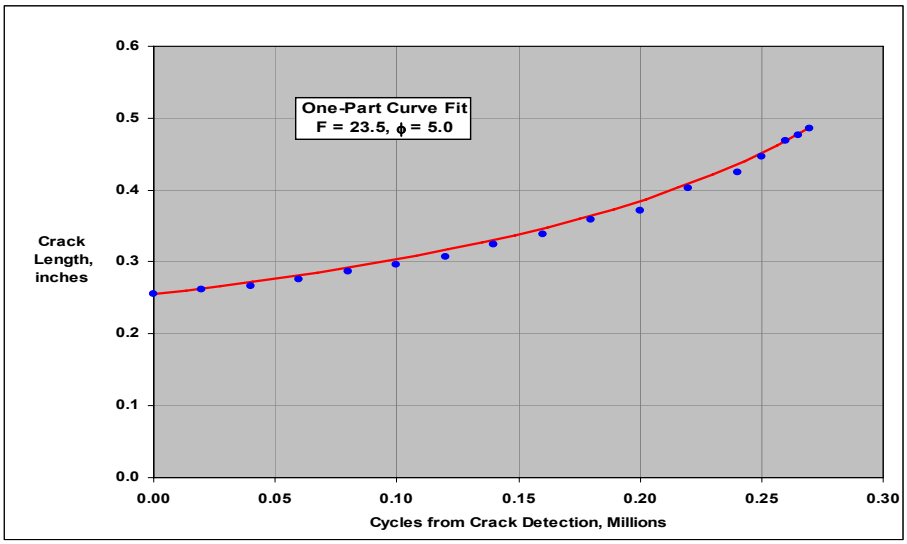

Figure 17: Aluminum Specimen 6 Crack Propagation Results

Good curve fits are obtained using the trial and error method. 4 of the 5 datasets require a two-segment curve fit, which is not unusual. The factors determined are summarized below.

Table 2: Aluminum Curve Fit Factors

Speci-men	Peak Load	Initial Crack Size, inches	Curve-Fit Factors				Switch Length, inches	Minimum Da/DN, inches/ cycle	Maximum Da/DN, inches/ cycle
			F1	ϕ1	F2	ϕ2			
2	2500	0.153	30.8	5.0	45.0	5.0	.456	2.8×10^{-7}	2.4×10^{-5}
3	3000	0.112	26.6	5.0	35.0	5.0	.416	2.8×10^{-7}	3.7×10^{-5}
4	1500	0.357	55.0	5.0	5200	10.0	.434	3.3×10^{-7}	4.7×10^{-6}
5	2500	0.318	26.0	5.0	180	10.0	.440	1.5×10^{-6}	2.3×10^{-5}
6	3000*	0.255	23.5	5.0	--	--	--	6.0×10^{-8}	9.6×10^{-6}

* Spectrum Loading

It can be seen that the factors for the first segment fits are in relatively good agreement – an exponent of 5 and F factors ranging from 23.5 to 55. While the range of more than 2:1 in F (life) may seem high, it is not unusual for full-scale crack propagation data. This scatter is one of the issues covered by the life reduction taken with full-scale test data to establish service inspection intervals, and it is mitigated to a significant degree by including multiple specimens in the full-scale test program.

The second segment curve fit agreement is relatively poor because Specimens 4 and 5 have a high degree of curvature over a short span, requiring an unreasonably high exponent to get a good fit. If Specimens 4 and 5 are constrained to have an exponent of 5, like the others, their F factors would be 79.0 and 35.5 respectively. The variation may just be another example of scatter, moving to a different region of the da/dN curve, or a change in load path as the crack grows rapidly. In any event, when all use the same exponent, the actual difference is small, is a second order effect in the steep region of the crack propagation near the end, and can be treated with a known degree of conservatism.

Additional conclusions on this data require reference to a material da/dN curve, shown below for 7075-T7351 aluminum, Figure 18. As a minimum the range of Da/DN values, as shown in Table 2, should be checked against the da/dN curve to assure that the testing is conducted in the "linear" range of the curve. For this comparison, the range of the possible "equivalent" threshold (i.e., in terms of crack growth rate, not ΔK) is sketched in using the estimated threshold line for R = 0.1 (no test data available at threshold). It is seen that all of the specimens are above this value, and also that none are into the unstable region at the high end of the curve.

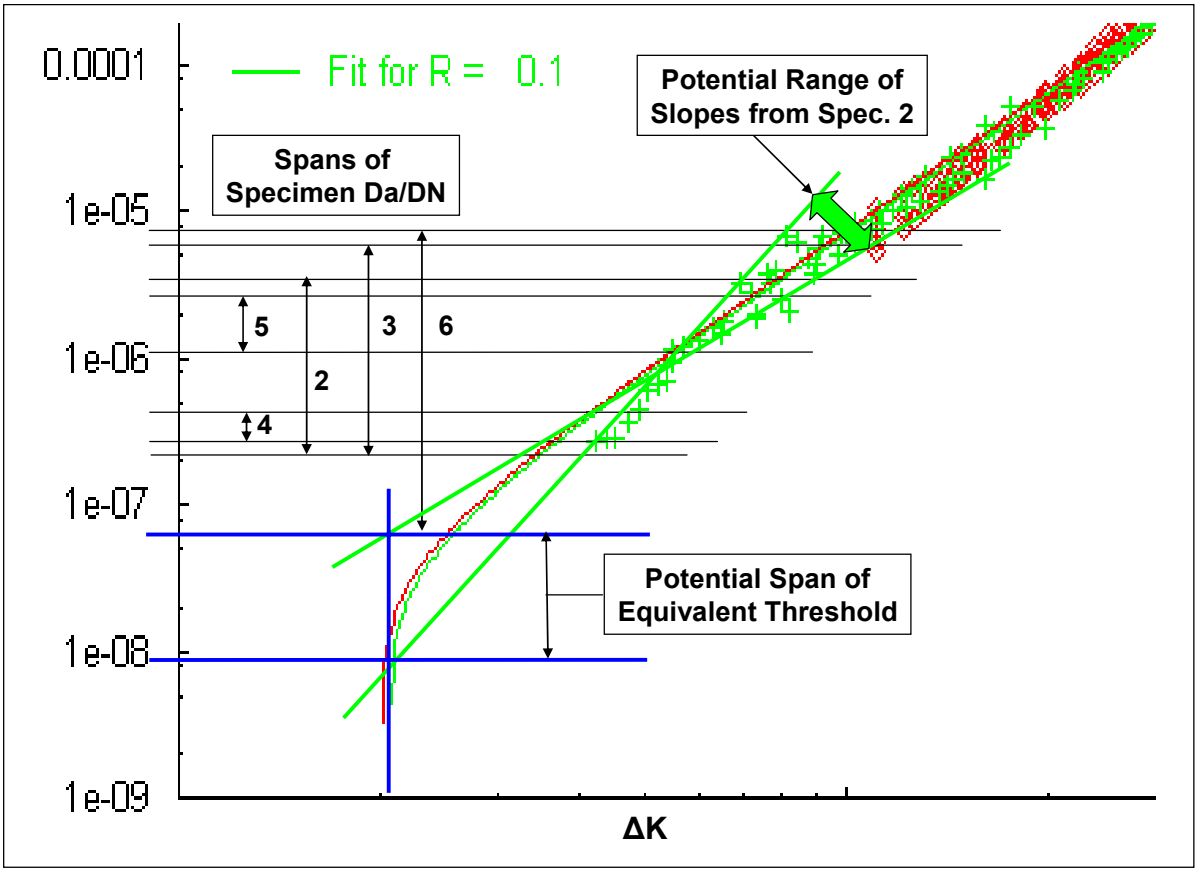

Figure 18: da/dN-ΔK Curve for 7075-T7351 Aluminum, with Annotations from Text

Additionally, this data can provide some valuable insights into how this component behaves at different loading conditions, and how effective the EDT method will be in predicting this behavior. Specifically, the EDT equation is based on the Paris Law and the assumption of a linear relationship on the log-log axes of a da/dN curve. But for this material, only one coupon specimen is available for the R-Ratio = 0.1 loading condition, green crosses on the figure. And a considerable variation in the growth rate over the crack length occurs for the one specimen. Differences of up to 3:1in crack growth rate can be seen in the area of interest.

The Da/DN span of each of the 5 specimens for the first segment of their curve fit is shown in the above figure. Since specimens 2 and 5 were tested at the same load, their average is chosen as a "baseline" for the exercise to "predict" the behavior of the other specimens. The specific growth lines for these two specimens are not known, since specific knowledge of ΔK is not available in the empirical method. However, their maximum and minimum growth rates place them in a region of high variability on the da/dN curve. A potential span of slopes that could result from specimen 2 is sketched in green.

4.3 Titanium propagation test data

Constant-amplitude crack growth testing was conducted on 4 titanium specimens and results were obtained as shown below in Figures 19-22. Crack lengths are corrected for edge distance. The applied loads used on the EDT curve fit process contain the correction determined in the strain surveys. Fit lines are shown for both a one-curve fit and a two-curve fit to illustrate the difference in approach.

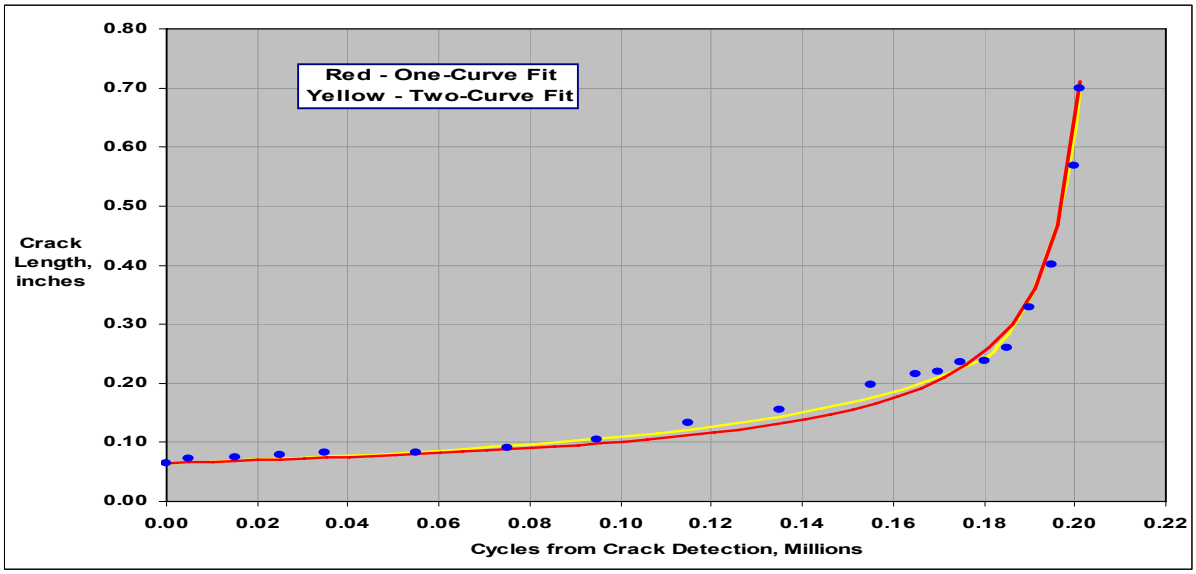

Figure 19: Titanium Specimen 1 Crack Growth Data and Curve Fits

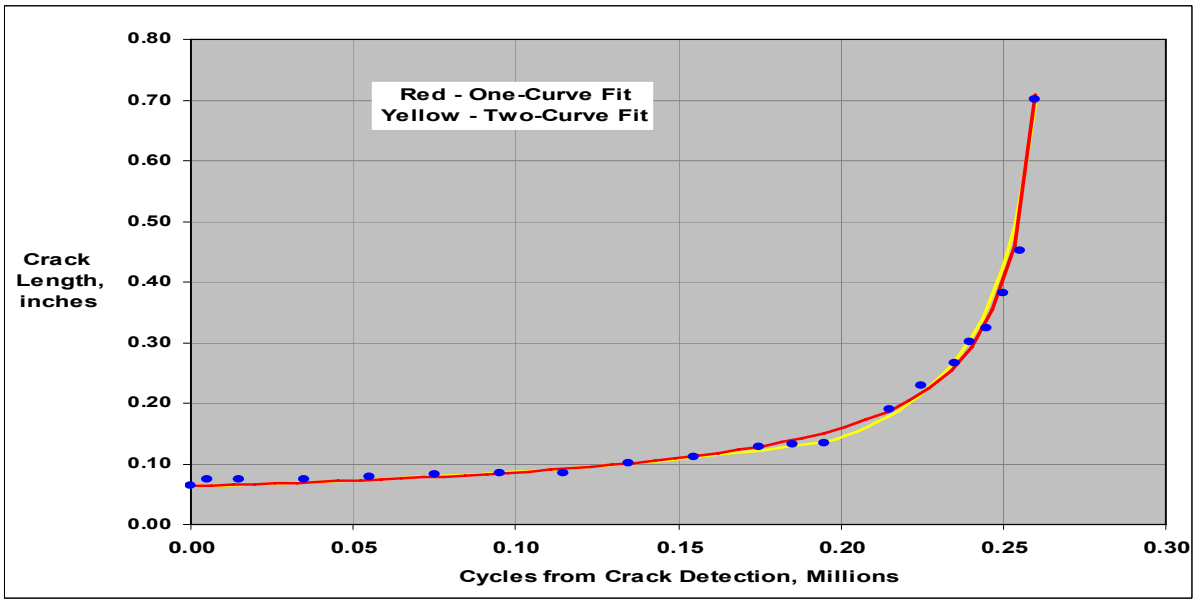

Figure 20: Titanium Specimen 2 Crack Growth Data and Curve Fits

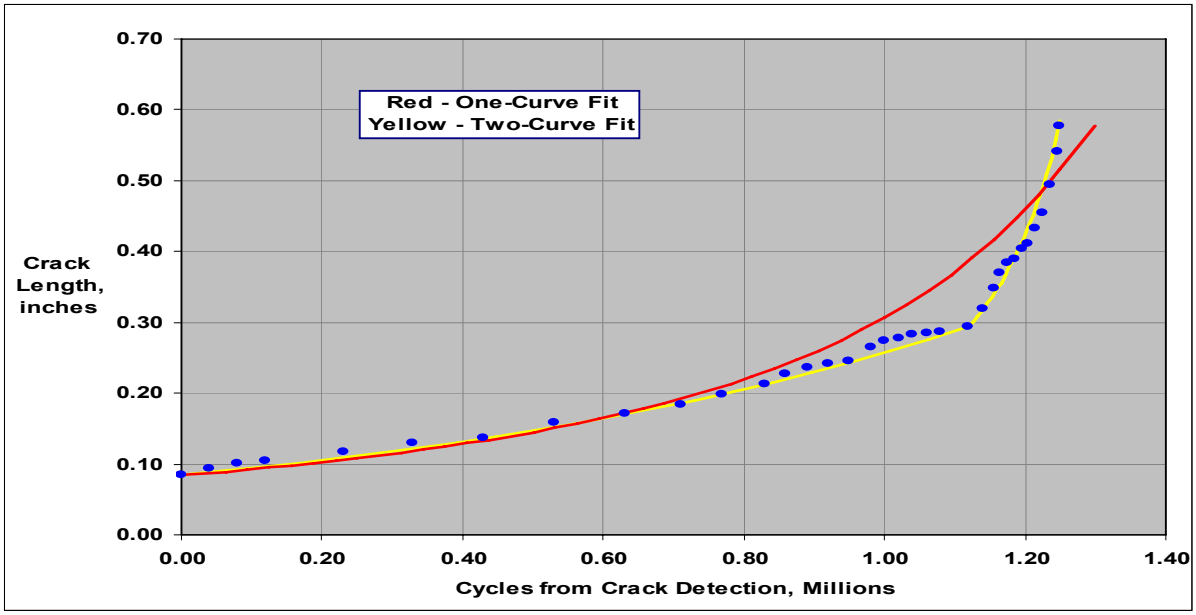

Figure 21: Titanium Specimen 3 Crack Growth Data and Curve Fits

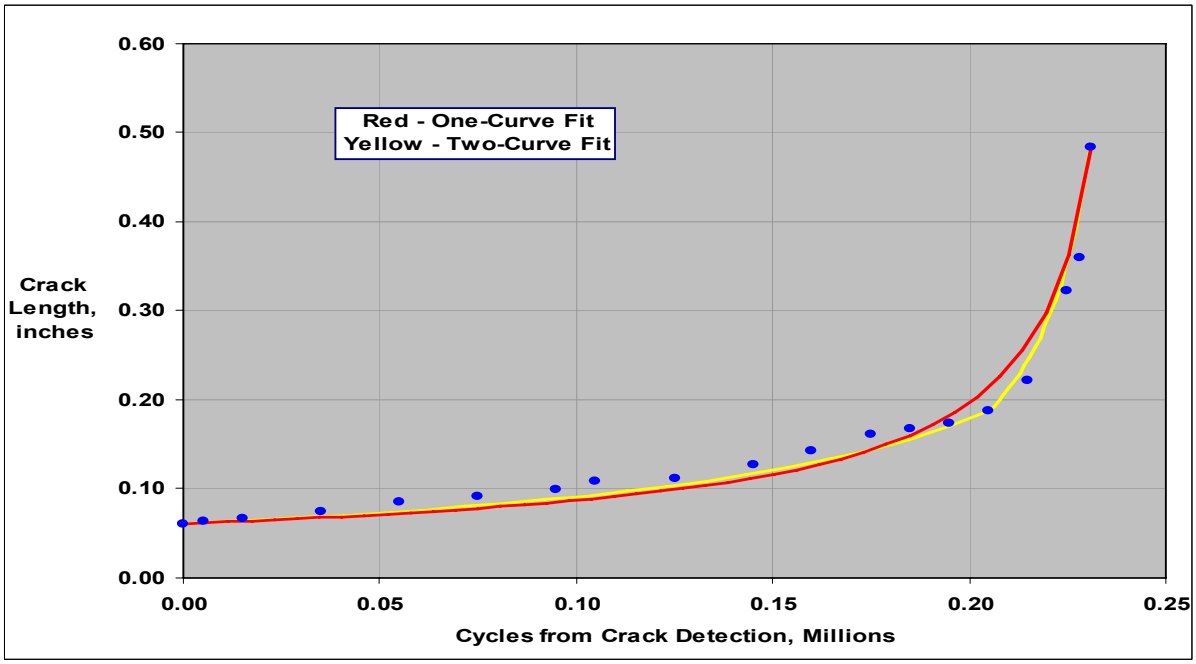

Figure 22: Titanium Specimen 4 Crack Growth Data and Curve Fits

Two-curve fits (yellow lines) were tried because of the distinct character change seen on Specimens 3 and 4. However, since this change was less distinct on Specimens 1 and 2, and also apparently occurred at a shorter crack length, a one-curve analysis (red lines) was selected for simplicity. These results are shown below in Table 3.

Table 3: Titanium Curve Fit Factors

Specimen	P_V	Initial Crack Size, inches	Curve Fit Factors		Minimum Da/DN, inches/ cycle	Maximum Da/DN, inches/ cycle
			F	ϕ		
1	1.13	0.065	106	5.0	$2.8x10^{-7}$	$8.0x10^{-5}$
2	1.0	0.112	158	5.0	$1.6x10^{-7}$	$6.5x10^{-5}$
3	0.67	0.084	11	3.0	$8.0x10^{-8}$	$1.4x10^{-6}$
4	1.0	0.318	183	5.0	$1.7x10^{-7}$	$3.0x10^{-5}$

The titanium results also include scatter. Specimen 3 is a relatively poor fit with a one-curve analysis, but an exponent of 5, like the others, produces an unconservative estimate for the early, important, part of the crack growth. An exponent of 3 minimizes this error. For reference, Specimen 3 with an exponent of 5 would result in an F-Factor of approximately 160. The other specimens have good fits with an exponent of 5, and relatively consistent F-Factors.

The Da/DN minimum and maximum values are again computed for comparison to the Material. da/dN curve, Figure 23 below.

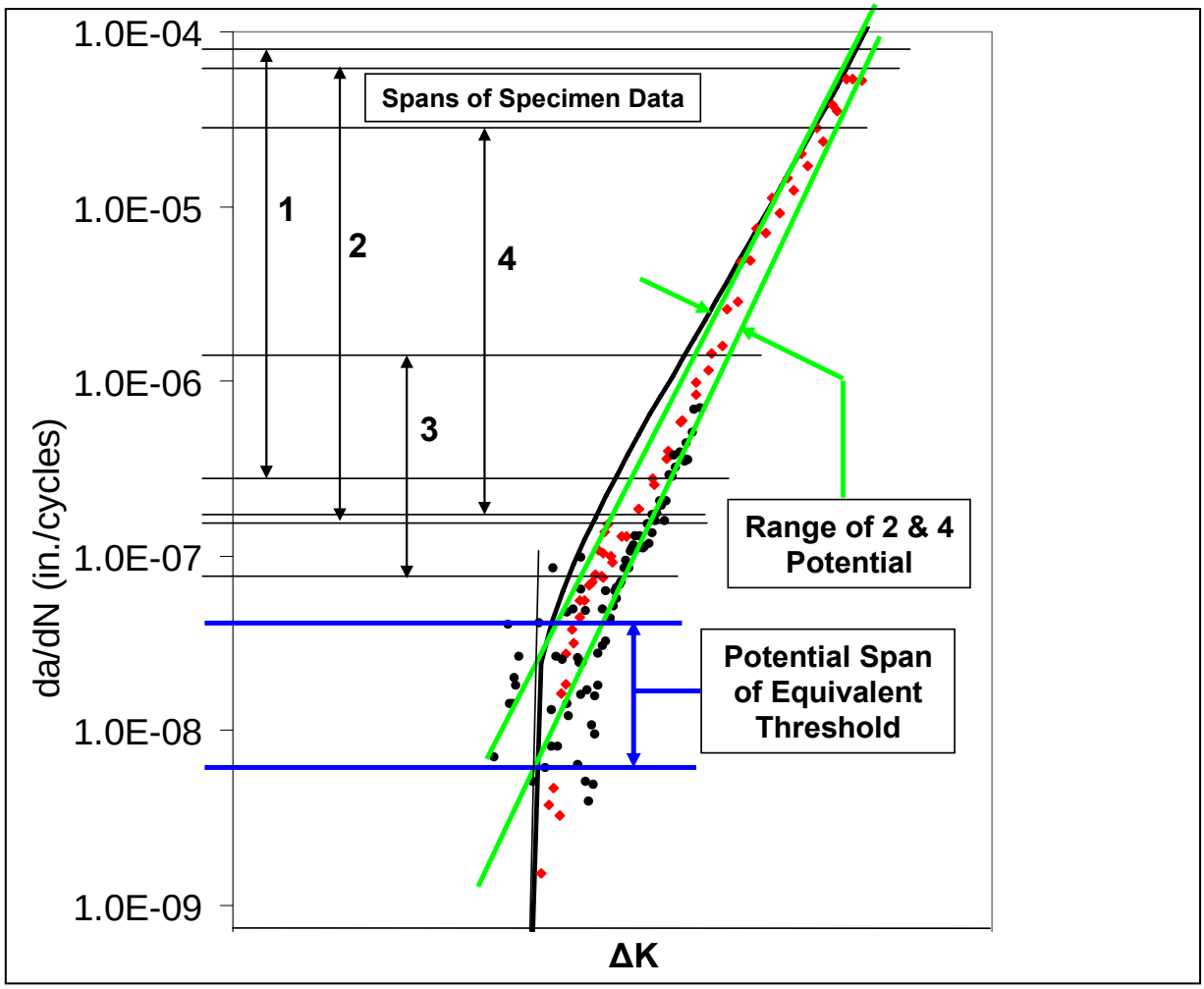

Figure 23: da/dN-ΔK Data for Ti-6Al-4V STOA Titanium at R = .1, with Annotations from Text

All are within the linear range to the curve, with Specimen 3 just over the highest equivalent threshold. Since this was a constant-amplitude test, the fact that it did propagate at that load and crack length provides an upper bound confirmation of the equivalent threshold.

Scatter and non-linearity issues are also evident for the titanium curve, even though it includes data from 5 coupon specimens. Predictions based on Specimens 2 and 4 could potentially result in errors of 3:1 in life. This potential is mitigated somewhat because the spans of the specimen da/dNs are longer and more coincident than with the aluminum data set. However, establishment of a credible equivalent threshold is difficult, even though the data set includes threshold points.

4.3 Actual vs. predicted for the aluminum data set

To establish a baseline for the prediction exercise, the results from Aluminum Specimens 2 and 5 are averaged, since they were tested at the same applied load, 2500 lb max. For the first part of the curve fit, both datasets have an exponent of 5, so the F-Factor can be just the average of the two, or 28.4. For the second part of the curve fit, Specimen 5 has the unrealistically high exponent to pick up the observed curvature of the high end data. In order to carry out an averaging process, a second curve fit to the high end of the Specimen 5 data was done with an exponent of 5. The resulting F-Factor is 35.5, and when averaged with the F-factor for Specimen 2 at the high end, 45.0, a baseline value of 40.3 is obtained.

A common point of switchover from the first curve fit to the second is also required. The average value from Specimens 2 and 5 of 0.448 inches was used.

The resulting baseline fit can be described in equation form:

a < 0.448”
$$\frac{Da}{DN} = 28.4\left(P_V \sqrt{a}\right)^{5.0} \quad (1)$$

a > 0.448”
$$\frac{Da}{DN} = 40.3\left(P_V \sqrt{a}\right)^{5.0} \quad (2)$$

These equations are numerically integrated using the P_V (applied load substantiating parameter) and initial crack size for each of the other 3 aluminum specimens, with results as shown below in Figures 24 – 26.

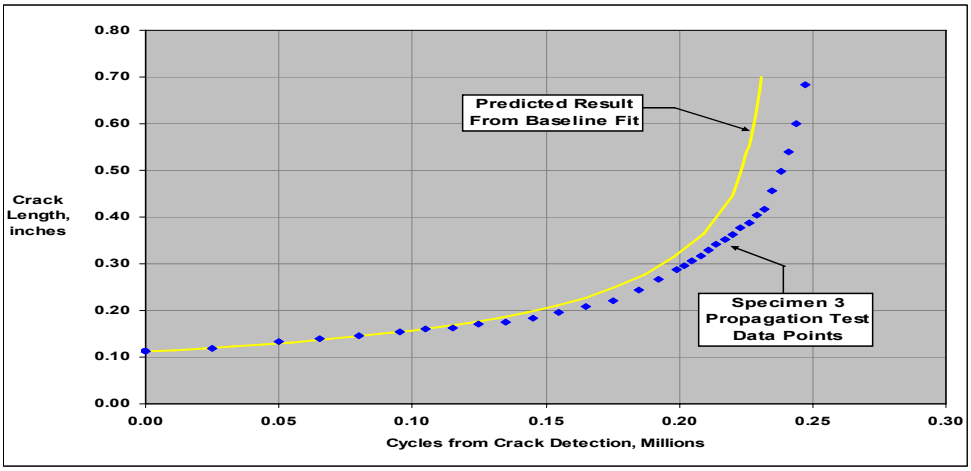

Figure 24: Comparison of Aluminum 3 Predicted and Actual Crack Propagation

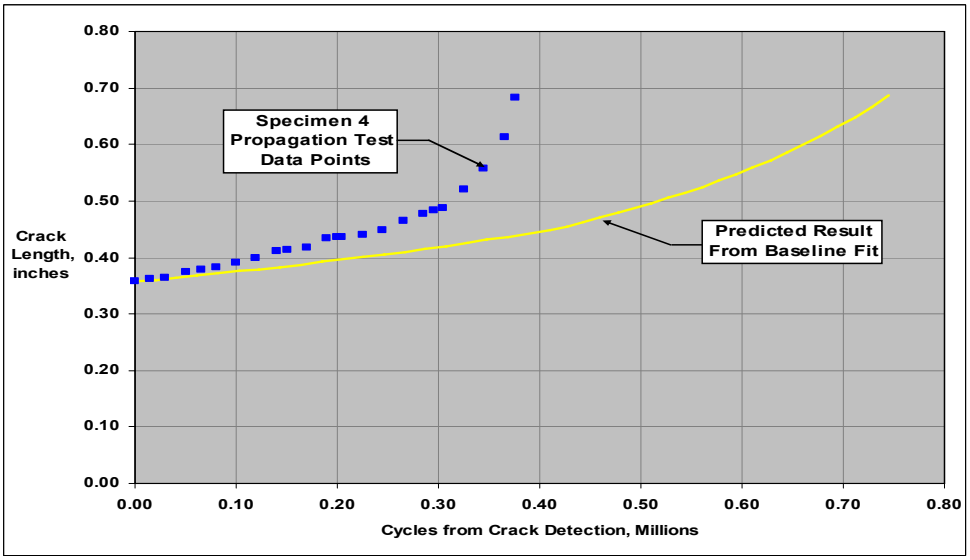

Figure 25: Comparison of Aluminum 4 Predicted and Actual Crack Propagation

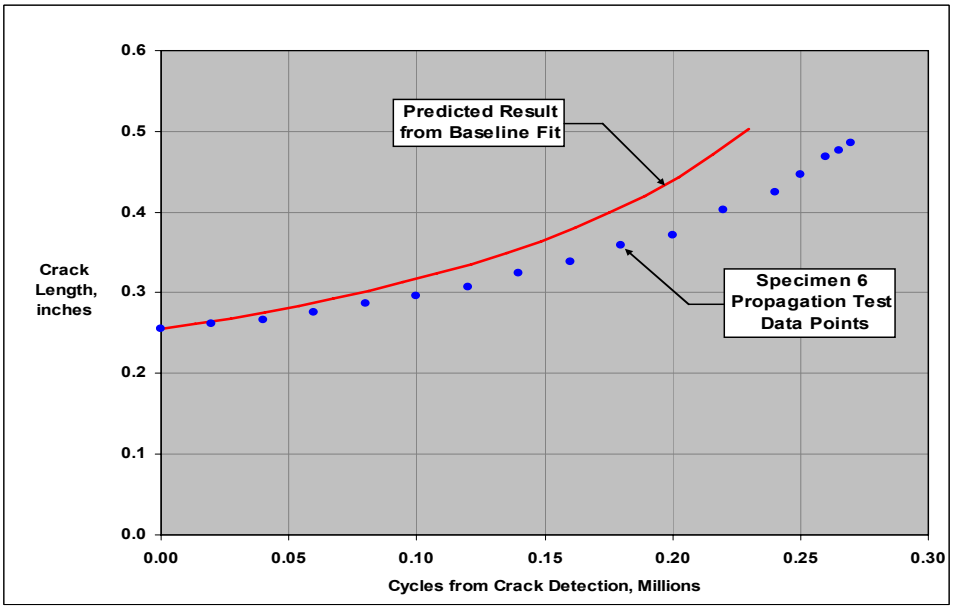

Figure 26: Comparison of Aluminum 6 Predicted and Actual Crack Propagation

Specimens 3 (constant amplitude) and 6 (spectrum) provide good results. The predictions are 6.5% and 17% low (conservative) respectively.

However, Specimen 4 is almost 2x high (unconservative). Figure 18 shows why this can happen – Specimen 4 has a very short span of da/dN and is in an area where the prediction can have a variation of 2x or more. This is the primary "lesson learned" from this study - namely that the normal scatter in crack propagation material characteristics can produce significant variations in a test-based prediction, up to 2:1 in life. However, the effect is covered by the normal 3:1 or 4:1 life margin in crack propagation time for service inspection intervals. In addition the effect can be significantly mitigated by testing multiple specimens over large spans of crack growth. Having a high-quality multiple-specimen material da/dN set also provides a major contribution to understanding what is happening in the full-scale test program.

4.4 Actual vs. predicted for the titanium data set

The baseline for the titanium data set is Specimens 2 and 4, both tested at 10,000 lb max load. Since they also have almost identical initial crack sizes, they can be plotted together without correction, Figure 27 below.

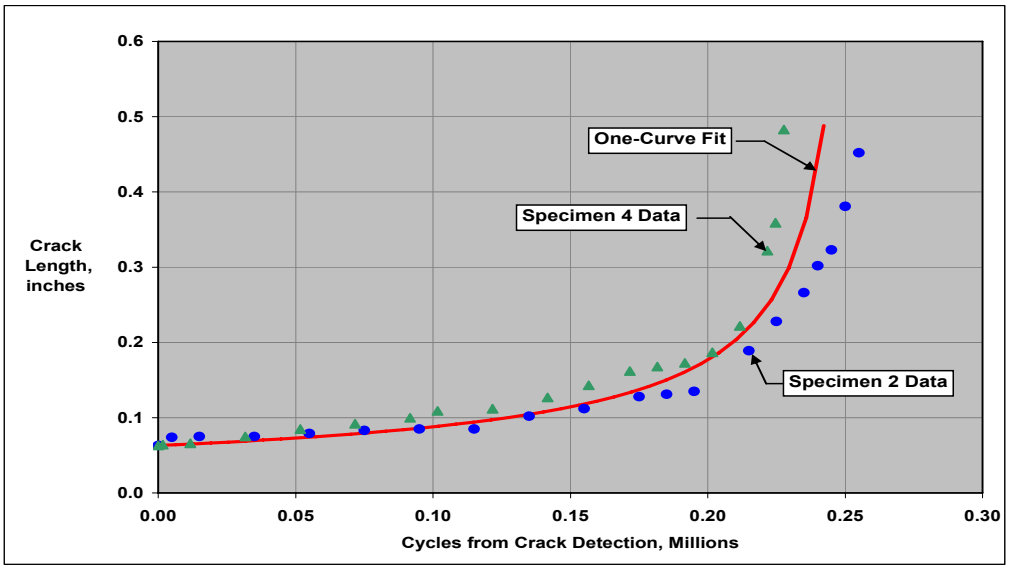

Figure 27: Titanium Specimens 2 and 4

The difference in these two data sets is 11% in life. A one-curve fit is selected for the baseline with parameters F = 166 and $\phi = 5.0$. An arithmetic average of the F-Factor for Specimens 2 and 4 is 170, but this figure does not produce as good an "average" fit. The baseline fit for the titanium specimens is therefore described by the EDT equation:

$$\frac{Da}{DN} = 166\left(P_V \sqrt{a}\right)^{5.0} \qquad (3)$$

Use of this equation to predict the result for Specimens 1 and 3 is shown in Figure 28 below.

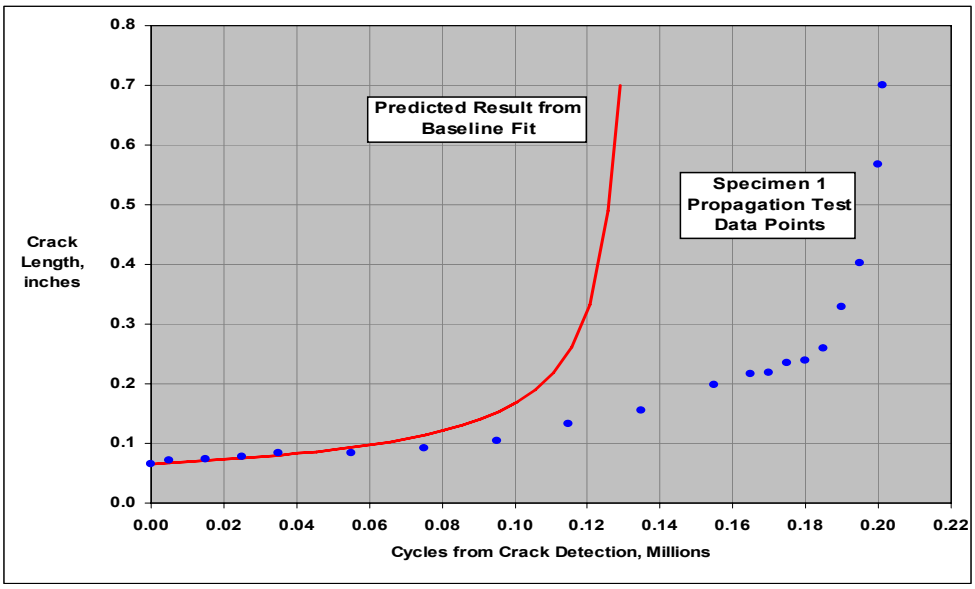

Figure 28: Comparison of Titanium 1 Predicted and Actual Crack Propagation

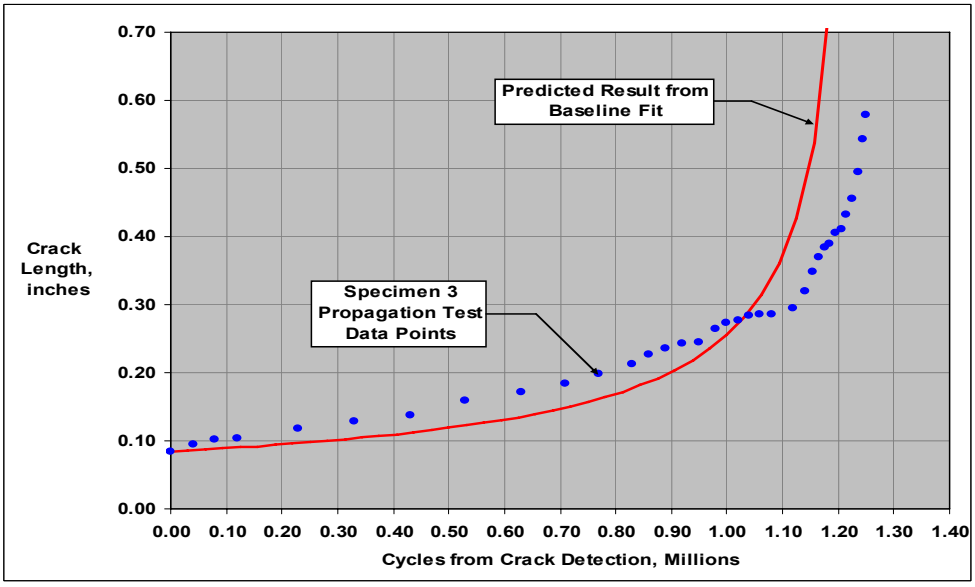

Figure 30: Comparison of Titanium 3 Predicted and Actual Crack Propagation

Specimen 1 is 35% low and Specimen 3 is 8% low (conservative), however, because of the poor fit to the baseline curve fit the Specimen 3 prediction is up to 20% high (unconservative) at the smaller crack sizes.

The insights from titanium results are similar to those from the aluminum work, plus the observation that propagation scatter can show up as a difference in curve shape fit as well as an error in the gross life determination.

5. DAMAGE TOLERANCE ANALYSIS

A crack growth analysis was conducted for Aluminum Specimen 3 at the high load condition, 3,000 lb applied peak load, R = 0.1. Based on the offset of the load from the centroid of the specimen cross-section, an axial plus bending stress at the crack location of 11.2 KSI is predicted. However, measurement of the maximum stress on the front face of the specimen showed only 9.8 ksi. This may be attributed to the inability of the spherical bearings and

pivot to allow the very small motions needed for the full bending stress to occur for small crack sizes. This observation points up another significant benefit of conducting full-scale crack propagation testing – the load distribution expected in design may not aloways occur, and a strain survey can provide a much more accurate value for the correlation of the analysis.

The crack growth analysis was conducted using NASGRO V4.22 using Sikorsky crack growth rate data (Figure 18). The initial crack was a corner crack at the edge of a plate, NASGRO CC01. The notch was modeled as a crack extending from the edge of the specimen. The justification is based on evaluations using stress intensity solutions established by Tada, Paris, and Irwin, Reference 4. Thus, a 0.065" deep initial crack at the 0.047" deep notch is modeled as an initial 0.112" deep crack from the edge. The analysis results are shown below:

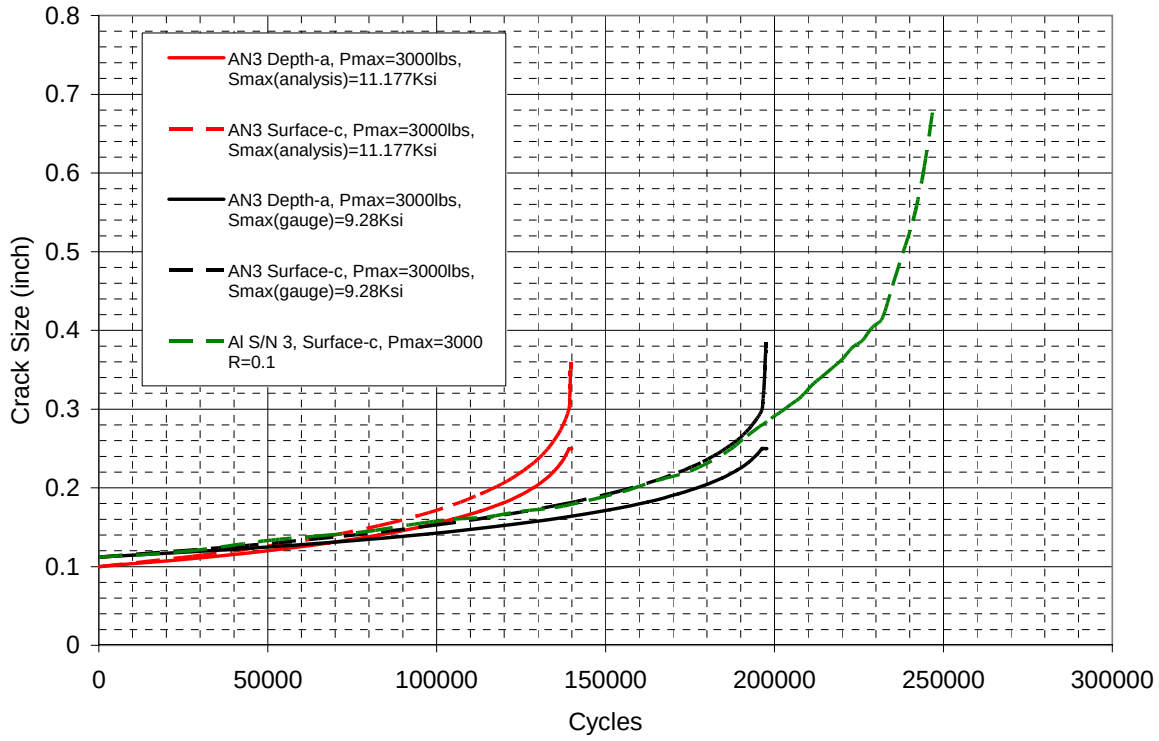

Figure 31. Crack growth Analysis for Aluminum Specimen 3, Peak Load = 3,000 lb

The red lines on this figure show the prediction for the nominal calculated surface stress of 11.2 Ksi, and results in a crack growth time of 140,000 cycles. The black lines show the prediction for the measured surface stress of 9.8 Ksi, and results in a crack growth time of 197,000 cycles. The green line is the propagation test data for Aluminum Specimen 3, with an actual crack growth time of 246,000 cycles.

Both analytical results are conservative, and safe, however, excessive conservatism is not a desired result since the resulting inspection interval could be too short to implement in service. Especially since even an accurate crack growth time could be marginally short in the first place.

The two analytical results also show the dramatic effect of having a good strain survey. With the strain survey, a relatively small error of 20% is obtained. Without the strain survey, the error is 43%.

It is also observed that the correlation of the actual result to the analysis with the strain survey is very good until the analysis predicts a change to very rapid growth to failure, at about .3" crack length. The actual result is flatter and continues to more that double that crack length and another 50,000 cycles. Potentially a more refined analysis could show a better result.

A crack growth analysis was also conducted for Titanium Specimen 1 at the high load condition, 12,000 lb applied peak load, R = 0.1. Based on the offset of the load from the centroid of the specimen cross-section, an axial plus bending stress at the crack location of 44.7 KSI is predicted. However, measurement of the stress on the front face of the specimen showed only 37.8 ksi, the same effect as seen in the aluminum specimen.

The crack growth analysis used the same methodology as the Aluminum specimen, with the crack growth rate data shown in Figure 23. A 0.029" deep initial crack at the 0.046" deep notch is modeled as an initial 0.075" deep crack from the edge. The analysis results are shown below:

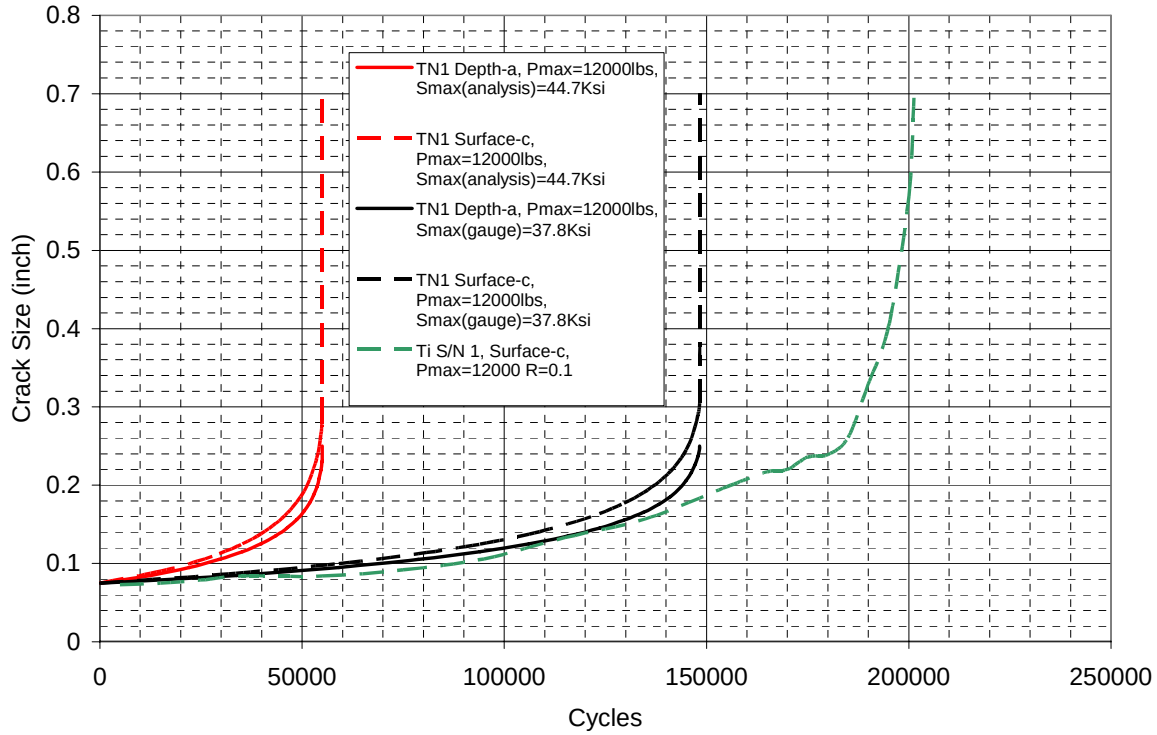

Figure 32. Crack growth Analysis for Titanium Specimen 1, Peak Load = 12,000 lb.

The red lines on this figure show the prediction for the nominal calculated surface stress of 44.7 Ksi, and results in a crack growth time of 55,000 cycles. The black lines show the prediction for the measured surface stress of 37.8 Ksi, and results in a crack growth time of 147,000 cycles. The green line is the propagation test data for Titanium Specimen 1, with an actual crack growth time of 202,000 cycles.

The same benefit of the strain survey is indicated for the Titanium Specimen. With the strain survey, a relatively small error of 25% is obtained. Without the strain survey, the error is 75%.

The same good correlation is seen until a rapid rise occurs in the analytical result starting at around .3" crack length.

6. CONCLUSIONS AND RECOMMENDATIONS

6.1 Conduct of crack propagation test programs

1. "Crack detection" gages can be an excellent method of catching a short crack, but use of strain gage bonding techniques are required to obtain good results.

2. If a "natural" fatigue crack is not available, the use of a machined groove and an EDM notch may be required to obtain a crack initiation at the point desired.

3. Measurement of crack length from a physical feature on the component, such as the edge where the crack is located, can provide an important contribution to the consistency of the crack growth data.

4. Test component loading must duplicate the aircraft loading and retain consistency as the crack grows. Multiple independent loads may be required.

6.2 Calibration of the Empirical Damage Tolerance method

1. The Empirical Damage Tolerance Method is validated, for the limited scope of this study, and within the bounds of scatter expected for crack propagation.

2. A good full-scale strain survey is required to choose and validate the test substantiating parameter. Use of the strain survey data can dramatically improve damage tolerance analytical results by removing the load distribution assumption.

3. Multiple full-scale test specimens are needed with this method, to assure that a conservative relationship is available for a range of load levels and to help compensate for scatter.

4. The process of curve-fitting to full scale crack propagation test data is not an exact process, and judgements are required in selecting a fit that is appropriate and conservative for the intended application.

5. High quality material da/dN data is required to understand the potential scatter in EDT predictions, to potentially correct the results, and to determine a conservative equivalent threshold. Use of an "analytical" threshold is not recommended.

6. The 3:1 minimum margin currently employed for full-scale test substantiations of inspection intervals appears appropriate for a multiple specimen EDT program with conservative loads and usage assumptions.

7. The Empirical Damage Tolerance method is ready for trial use. However, additional development and understanding is still necessary, and will inevitably occur with experience.

REFERENCES

[1] P.E. Irvin, J. Lin, and J.W. Bristow, "*Damage Tolerance in Helicopters, Report on the Round Robin Challenge*", American Helicopter Society 59th Annual Forum, Phoenix, Arizona, May 2003.

[2] D.O. Adams and D.E. Tritsch, "*Empirical Damage Tolerance*", American Helicopter Society 61st Annual Forum, Grapevine, Texas, June 2005.

[3] P.C. Paris and F. Endogen, "*A Critical Analysis of Crack Propagation Test Laws*", Jour. Basic Eng. 85, pp 528-534, 1963.

[4] H. Tada, P.C. Paris, and G.R. Irwin , "*The Stress Analysis of Cracks Handbook"*, Wiley, 1973, pp19.13